Journal of the Serbian Chemical Society
JSCS-info@shd.org.rs • www.shd.org.rs/JSCS

J. Serb. Chem. Soc. 85 (5) 671–685 (2020)
JSCS–5330

Original scientific paper

Preparation of $FePO_4{\cdot}2H_2O$ from $LiFePO_4$ mixed with $LiNi_xCo_yMn_{1-x-y}O_2$ waste material

HONGHUI TANG[1,2], YANCHAO QIAO[2], XI DAI[1]*, FENG TAN[2] and QIANG LI[2]

[1]*School of Metallurgy and Environment, Central South University, 410083 Changsha, Hunan, P. R. China and* [2]*Hunan Brunp Recycling Technology Co., Ltd, 410600 Ningxiang, Hunan, P. R. China*

(Received 16 September 2019, revised 10 January, accepted 16 January 2020)

Abstract: A method for preparing battery grade $FePO_4{\cdot}2H_2O$ from $LiFePO_4$ and $LiNi_xCo_yMn_{1-x-y}O_2$ mixed waste is proposed. The optimum leaching conditions included: temperature of 50 °C, 3:1 liquid–solid mass ratio, 3.6 HCl/$FePO_4{\cdot}2H_2O$ mole ratio, 0.75 H_2O_2/$FePO_4{\cdot}2H_2O$ mole ratio, and 2 h reaction time. The solution obtained from the leaching waste material was diluted to a 1.0 M Fe concentration, then transferred to an 1 L beaker, where temperature, pH, complexing agent, ammonia addition rate and feeding mode were studied in order to determine their effects on the precipitation, particle size and morphology of $FePO_4{\cdot}2H_2O$. High precipitation rate of Fe with low percentages of Al, Ni, Co, Mn in the $FePO_4{\cdot}2H_2O$ is achievable when precipitation is performed at a temperature of 85 °C, pH of 2.0, and 20 g L^{-1} complexing agent. Furthermore, it was observed that a slow addition of ammonia and a flow feeding method contributed to the production of $FePO_4{\cdot}2H_2O$, with small particle sizes and a flake morphology.

Keywords: spent materials; complexing; preparation; $FePO_4{\cdot}2H_2O$.

INTRODUCTION

Lithium-ion batteries have been widely used since the first successful commercialisation in the 1990s.[1,2] This is due to their superior performance,[3,4] which includes high specific energy, long cycle life, safety, and lack of memory effects.[5–7] Lithium iron phosphate batteries and lithium nickel cobalt manganese oxide batteries may be the most common lithium-ion batteries.[8,9] Due to the limited service the life of lithium-ion batteries, their development and use resulted in a large number of scrapped batteries, and this constitutes a waste of resources (such as Li, Fe, Ni, Co, Mn, Al and other metals) if not managed properly.[10] Moreover, the presence of harmful substances could lead to serious

* Corresponding author. E-mail: luckcici1596@163.com
https://doi.org/10.2298/JSC190916005T

environmental damage. Therefore, the development of an effective technology for recycling lithium-ion batteries has attracted worldwide attention.[11,12]

Currently, lithium-ion battery recycling methods include echelon use, fire recovery, wet leaching, bioleaching, and regeneration.[13–17] Duke Energy cooperated with ITOCHU Corporation to conduct a series of tests on waste batteries that could not be used as automobile power batteries because their capacity was less than 80 % of original, and they analysed the service data in order to determine possible fields of application for the products.[18] Li *et al.* added Li_2CO_3 to the waste materials and the resultant mixture was regenerated at 650 °C, after which the discharge specific capacity and coulombic efficiency were 140.4 mA h/g and 95.32 % after 100 weeks of cycling, respectively; this would meet the requirements for lithium-ion batteries.[19]

Many methods for preparing $FePO_4{\cdot}2H_2O$ have been reported, including coprecipitation, hydrothermal, spray drying, homogeneous precipitation and oxidation–liquid phase precipitation. Kandori *et al.* prepared a number of ultrafine phosphates with good particle size uniformity and high purity by homogeneous coprecipitation.[20] Mal *et al.* used ferric chloride and sodium phenyl phosphate as the iron source and phosphorus source, and sodium dodecyl sulphate as the surfactant, and successfully prepared composite medium $FePO_4$.[21] However, these methods require very pure raw materials.

There are a few reports on the preparation of $FePO_4{\cdot}2H_2O$ from waste $LiFePO_4$; Bian *et al.* prepared an $FePO_4{\cdot}2H_2O$ precursor by a heated crystallization and solvothermal method. After dissolving $LiFePO_4$ waste with acid, supplemented with Li_2CO_3 and glucose, $LiFePO_4$/C cathode material was re-synthesised after heat treatment and it resulted in a new material that meets application requirements.[22] It should be noticed that the $LiFePO_4$ waste used for research must not contain impurities.

However, the impurities of Ni, Co, Mn are often detected in $LiFePO_4$ waste, some of them doped into the material and some present as a mixture of $LiNi_xCo_yMn_{1-x-y}O_2$ and $LiFePO_4$. In the production of batteries, acetylene black (as a conductive agent), PVDF (as a binder), and a cathodic material were generally mixed and pulped, while $LiFePO_4$, a poor conductor, was coated with carbon to improve electrical conductivity and low-temperature performance; therefore, it is inevitable that carbon would be present in the cathodic material. An aluminium piece was used to support the cathodic material and was extremely difficult to remove it during the recycling process, causing a challenge for subsequent separation and purification.[23] To our knowledge, there are few papers that report processes for the preparation of $FePO_4{\cdot}2H_2O$ from $LiFePO_4$/ /$LiNi_xCo_yMn_{1-x-y}O_2$ waste material.

In this work, a small amount of $LiNi_xCo_yMn_{1-x-y}O_2$ waste was artificially incorporated into $LiFePO_4$ waste to simulate the composition of lithium iron

phosphate waste. The purpose was to prepare $FePO_4{\cdot}2H_2O$ from $LiFePO_4$/ /$LiNi_xCo_yMn_{1-x-y}O_2$ waste material, and we report the effects of temperature, pH, Fe/P molar ratio, complexing agent, ammonia addition rate, and feeding mode on the purity, composition, morphology and particle size of the resultant battery-grade $FePO_4{\cdot}2H_2O$, which was identified in accordance with the HG/T 4701-2014 standard.

EXPERIMENTAL

Materials

Spent materials of $LiFePO_4$ mixed with $LiNi_xCo_yMn_{1-x-y}O_2$ were provided by a recycling company in Hunan, China. The materials were washed, dried and aluminium was removed by NaOH solution via ball milling to obtain the desired material. The process is shown as follows:

$$2Al + 2NaOH + 2H_2O \rightarrow 2NaAlO_2 + 3H_2\uparrow \quad (1)$$

Chemical and phase compositions and morphology were determined and results detailed in Results and discussion.

Analytical grade reagents used were HCl (36–38 %), H_2O_2 (30 %) and EDTA-2Na (purity > 99 %), obtained from Sinopharm Chemical Reagent Co. LTD, China; NaOH (purity > 96 %) and $NH_4H_2PO_4$ (purity > 99 %) from Xilong Scientific Co. LTD, China; and $NH_3{\cdot}H_2O$ (25–28 %) from Hunan Hengyang Kaixin Chemical Co. LTD, China. Deionised water was used to prepare the solutions.

Experimental apparatus and procedure

A schematic diagram of the experimental setup is shown in Fig. 1. A replica reactor (1 L beaker with a baffle) was used and maintained at constant temperature. The baffle eliminates swirling, enhances stirring, and increases transfer efficiency.[24-26]

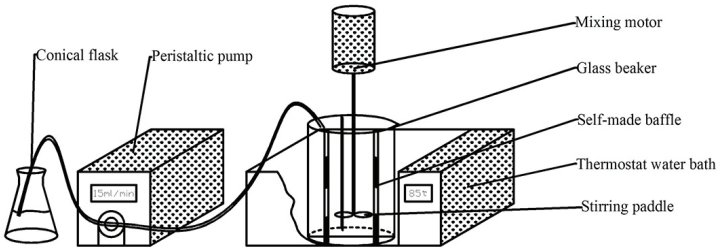

Fig. 1. Schematic diagram of experimental setup.

The mixed waste was leached with HCl and H_2O_2, and influence of temperature (30-70 °C), liquid/solid ratio (2–4), reaction time (1–3 h), HCl/raw material ratio (0.98–2.28 ml g^{-1}) and H_2O_2/raw material ratio (0–0.4 ml g^{-1}) on leaching efficiency was investigated (Table I). Leaching efficiency was calculated using Eq. (2):

$$\text{Leaching rate, \%} = 100\frac{m_2 - m_1}{m_2} \quad (2)$$

where m_1 = total amount of a specific element in the solid after leaching and m_2 = total amount of this element in the solid before leaching.

TABLE I. Experimental conditions of the leaching experiment

Experimental group	T °C	Liquid/solid ratio	$c_{HCl\ (36\ \%)}$ ml g^{-1}	$c_{H_2O_2\ (30\ \%)}$ ml g^{-1}	t / h	Variable
A	–	3:1	1.96	0.24	1.5	Temperature
B	50	–	1.96	0.24	1.5	Ratio of liquid to solid
C	50	3:1	–	0.24	1.5	HCl
D	50	3:1	1.96	–	1.5	H_2O_2
E	50	3:1	1.96	0.24	2.0	Reaction time

The solution obtained at optimal leaching conditions was diluted to obtain 1.0 M Fe and the resulting solution (diluted leached solution) was used for $FePO_4{\cdot}2H_2O$ precipitation. The volume of diluted leached liquid used was 400 mL. The experiment was conducted in two parts: 1) in one-way feeding, the diluted leached solution was transferred to the 1 L beaker and the aqueous ammonia was gradually added with constant heating and stirring to adjust the pH; and the reaction continued for 4 h after ammonia addition and 2) in concurrent feeding, pure water was added to the beaker and stirred. Then, the diluted leached solution and aqueous ammonia were pumped into the beaker simultaneously, using a peristaltic pump. The pH was determined and the reaction continued for 4 h. The solids were then separated from the slurry by filtration, washed by deionised water three times, dried at 80 °C, and the $FePO_4{\cdot}2H_2O$ product was isolated. The effects of temperature (55–95 °C), final pH (1.5–2.5), Fe/P mole ratio in solution (from 1:1 to 1:1.65) and complexing agent (0–40 g L^{-1}) on the characteristics (Fe/P ratio, Al, Ni, Co and Mn content in the product and precipitation rate) of $FePO_4{\cdot}2H_2O$ was determined (Table II).

TABLE II. Experimental conditions of the precipitation of $FePO_4{\cdot}2H_2O$; feeding mode: one-way

Experimental group	T °C	Final pH	Fe/P mole ratio	$c_{Complexing\ agent}$ g L^{-1}	Time of ammonia addition, min	Variable
1	–	2	1:1.2	0	30	Temperature
2	85	–	1:1.2	0	30	Final pH
3	85	2	–	0	30	Mole ratio of Fe/P
4	85	2	1:1.2	–	30	Complexing agent

The calculation method of precipitation rate as shown in Eq. (3):

$$\text{Precipitation rate, \%} = 100\frac{m_4 - m_3}{m_4} \tag{3}$$

where m_3 = total amount of a specific element remaining in liquid after precipitation and m_4 = total amount of the element in liquid before precipitation.

Analytical and testing methods

In the analysis of raw materials and products, chemical analysis and inductively coupled plasma optical emission spectrometry (Thermo Scientific iCAP 7200 ICP-OES) were used to determine the composition. A 0.2000 g sample was dissolved in minimal *aqua regia*, and the

resulting solution cooled and adjusted to a 250 mL volume, then diluted to a concentration within the measurable range of the sample curve, and the concentration of the element determined by ICP-OES. Liquid samples were acidified to pH < 2.0 with dilute nitric acid, the solution diluted to within a measurable range, and the corresponding element concentration determined by ICP-OES. X-ray diffraction (XRD, Ultima IV, step: 0.004°, step time: 23.8 s, start: 5.000°, end: 70.008°) and scanning electron microscopy (SEM-EDS, Nova NanoSEM450) were used to determine the mineralogical composition, micromorphology, and distribution of elements. Laser particle size analyser (LPSA, Mastersizer 3000) was used to determine granularity.

RESULTS AND DISCUSSION

Characterization and processing of raw materials

The results of chemical analyses of spent materials are listed in Table III, while the XRD pattern and granularity data, and electron microscope analysis (SEM) results of the raw materials are shown in Figs. 2 and 3, respectively.

TABLE III. Main chemical composition of $LiFePO_4$ mixed with $LiNi_xCo_yMn_{1-x-y}O_2$ waste materials

Component	Fe	P	Al	Li	Ni	Co	Mn
c / wt.%	28.54	15.81	0.02	3.62	0.56	0.38	0.39

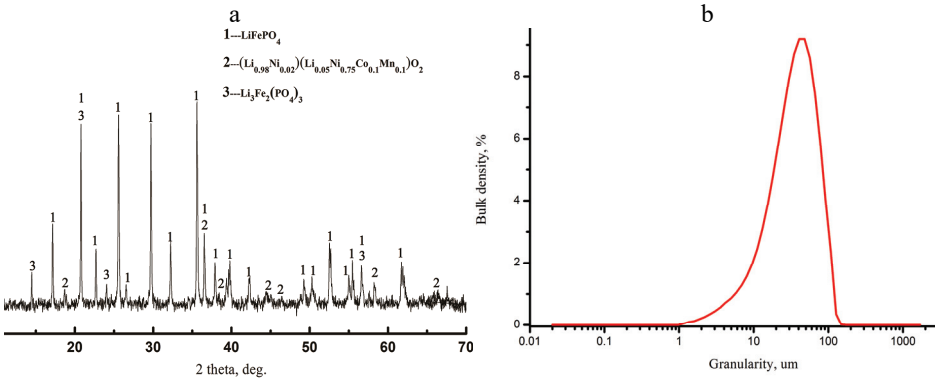

Fig. 2. XRD (a) and granularity (b) of $LiFePO_4$ mixed with $LiNi_xCo_yMn_{1-x-y}O_2$ waste materials.

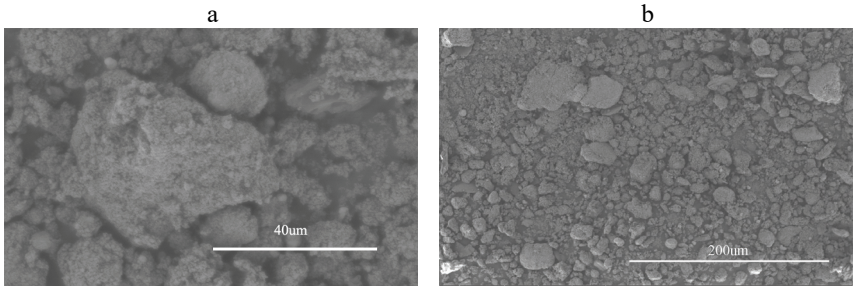

Fig. 3. SEM of $LiFePO_4$ mixed with $LiNi_xCo_yMn_{1-x-y}O_2$ waste: a) 5000×; b) 1000×.

The main elements in $LiFePO_4/LiNi_xCo_yMn_{1-x-y}O_2$ waste materials were Fe, P, and Li, and the major species was presumed to be $LiFePO_4$ containing small amounts of metal impurities such as Ni, Co, and Mn (Table III). The XRD pattern (Fig. 2a) indicated that the main species present were $LiFePO_4$, $LiNi_xCo_yMn_{1-x-y}O_2$ and $Li_3Fe_2(PO_4)_3$, where $Li_3Fe_2(PO_4)_3$ resulted from the oxidation of $LiFePO_4$. The particle sizes of the raw material were uniform and the average size was <50 mm (Figs. 2b and 3); thus making it unnecessary to consider the effects of particle size on leaching. EDS analysis showed that the surface of the raw material contained O, Fe, P, Mn, Ni, and Co (Fig. 4). Additionally, it was observed that Ni, Co, and Mn in the raw materials were evenly distributed.

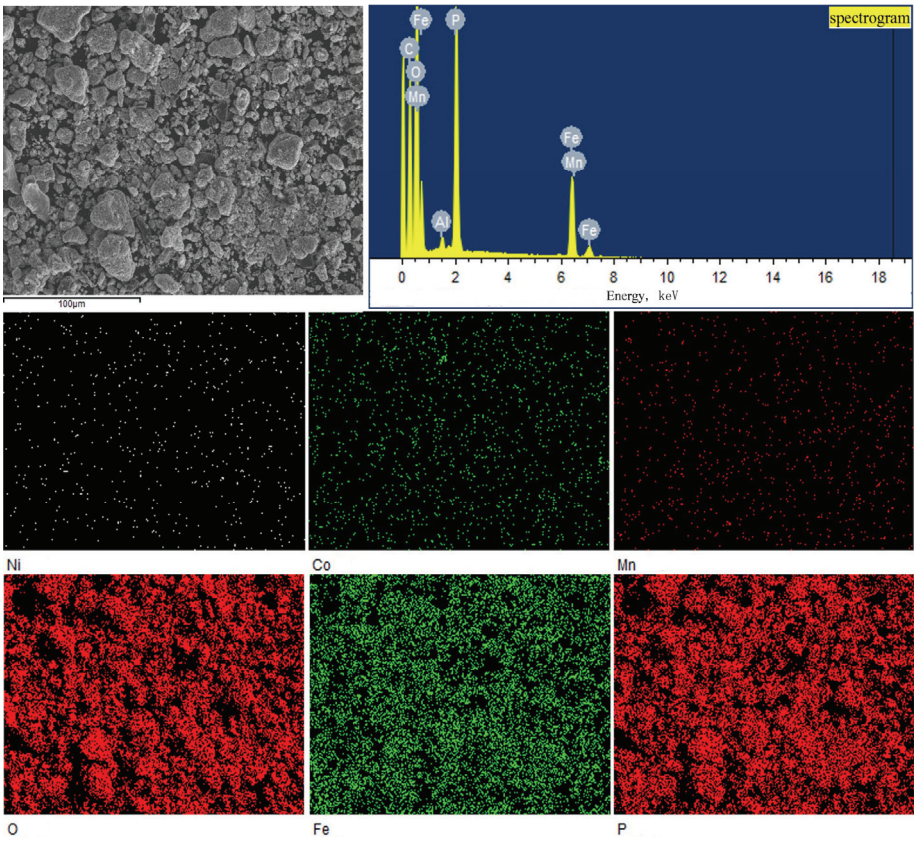

Fig. 4. SEM-EDS analysis of $LiFePO_4/LiNi_xCo_yMn_{1-x-y}O_2$ waste materials.

Preparation of solution

The $LiFePO_4$/ $LiNi_xCo_yMn_{1-x-y}O_2$ waste materials were treated with HCl–$-H_2O_2$ for leaching (Fig. 5).

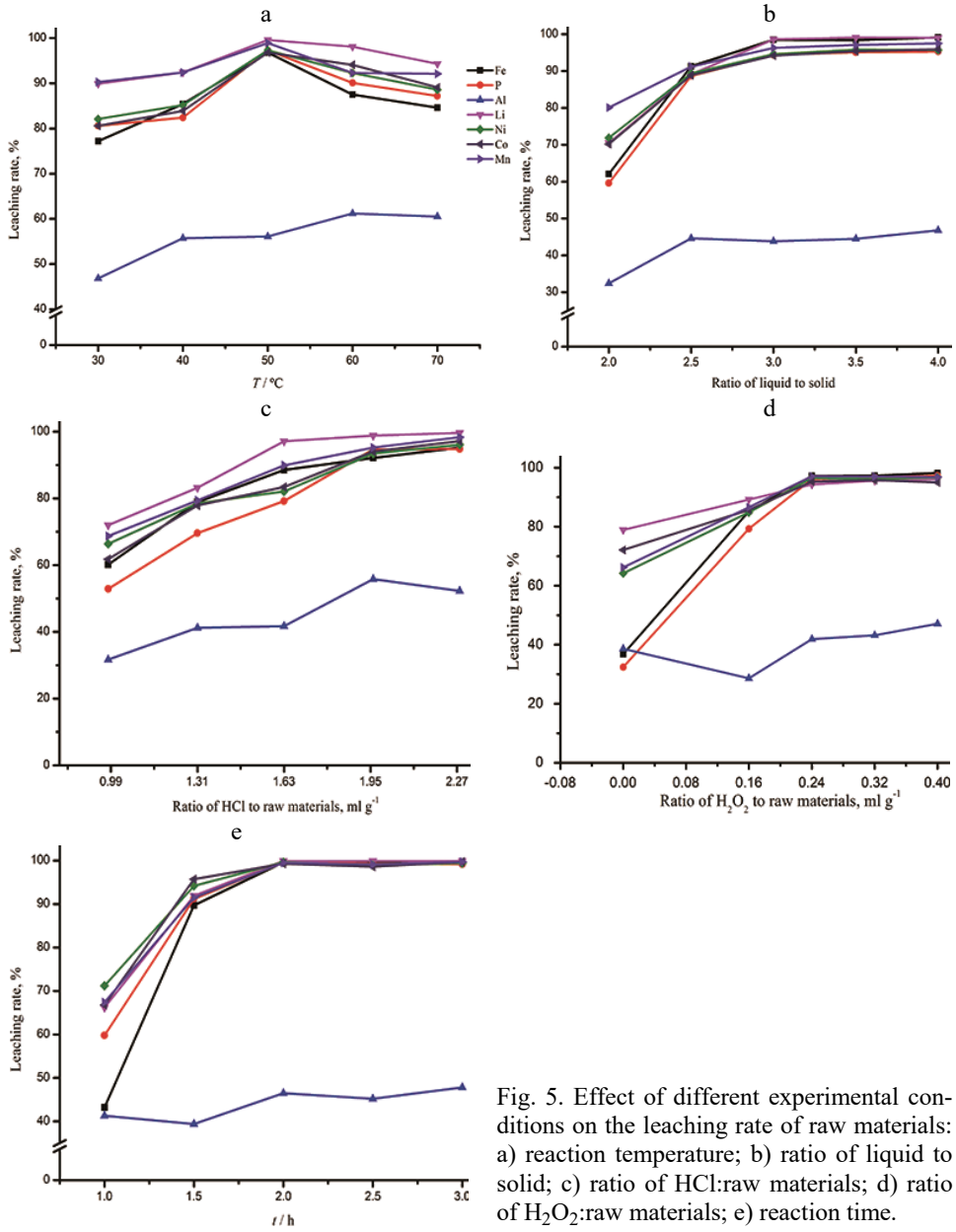

Fig. 5. Effect of different experimental conditions on the leaching rate of raw materials: a) reaction temperature; b) ratio of liquid to solid; c) ratio of HCl:raw materials; d) ratio of H_2O_2:raw materials; e) reaction time.

The optimum process conditions were as follows: temperature, 50 °C; liquid–solid ratio, 3:1; HCl/raw material ratio, 1.96 ml g^{-1}, H_2O_2/raw material ratio, 0.24 ml g^{-1}; reaction time, 2 h (Fig. 5). The leaching efficiency of Li, Fe, P, Ni, Co and Mn was more than 99.3 %.

HCl leaching of $LiFePO_4/LiNi_xCo_yMn_{1-x-y}O_2$ waste materials may be represented by the following reactions:

$$2LiFePO_4 + 6H^+ + H_2O_2 \rightarrow 2Li^+ + 2Fe^{3+} + 2H_2PO_4^- + 2H_2O \quad (4)$$

$$2LiNi_xCo_yMn_{1-x-y}O_2 + 6H^+ + H_2O_2 \rightarrow 2Li^+ + 2xNi^{2+} + 2yCo^{2+} + \\ + (2-2x-2y)Mn^{2+} + 4H_2O \quad (5)$$

After the dilution of the leached solution to 1.0 M Fe, the elemental composition of the dilution leached liquid was determined (Table IV).

TABLE IV. Composition of diluted leached solution of $LiFePO_4$ mixed with $LiNi_xCo_yMn_{1-x-y}O_2$ waste materials

Component	Fe	P	Al	Li	Ni	Co	Mn
c / g L^{-1}	55.84	30.90	0.013	6.90	1.09	0.73	0.76

Preparation of $FePO_4 \cdot 2H_2O$

Effect of temperature. The Fe/P molar ratio in the product was largely unaffected by reaction temperature, whereas Al, Ni, Co and Mn concentrations decreased with increasing reaction temperature (Fig. 6). The crystallinity of the product obtained at 95 °C was higher than the one obtained at 55 °C (Fig. 7). The 55 °C product was largely amorphous, with virtually no diffraction peaks in the spectrum; presumably, the amorphous structure could adsorb more impurities due to the high activity. Henceforth, the content of Ni, Co, Mn and Al in this $FePO_4$ were high. The $FePO_4 \cdot 2H_2O$ obtained at 95 °C had sharp peak shapes and good crystallinity, and the amount of Ni, Co, Mn and Al impurities entering the crystal lattice were reduced because of the high crystallinity. From related studies, we conclude that 85 °C is the optimal leaching temperature and it results in lower amounts of Ni, Co, Mn and Al in the $FePO_4$ product.

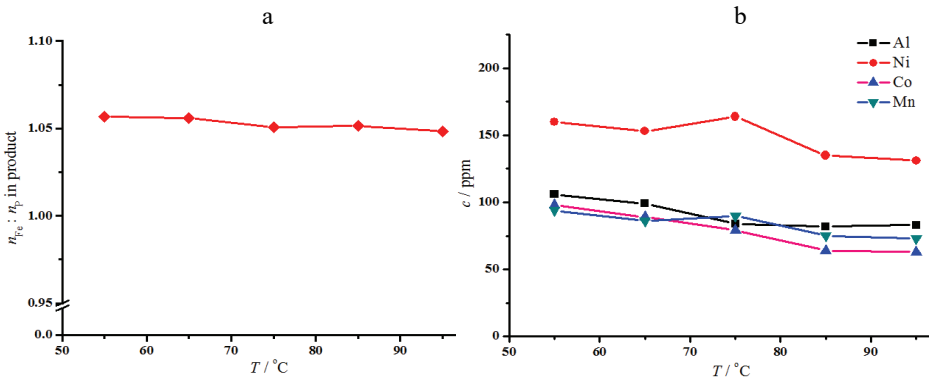

Fig. 6. a) Effect of reaction temperature on Fe/P mole ratio; b) effect of reaction temperature on Al, Ni, Co and Mn content.

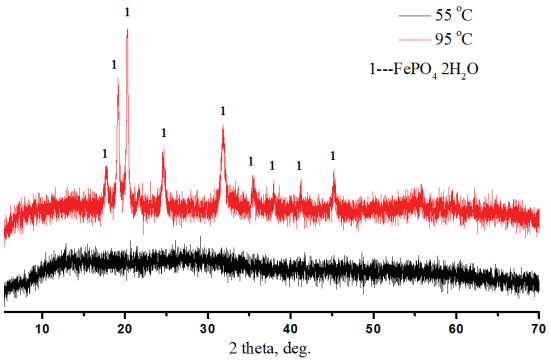

Fig. 7. XRD pattern of $FePO_4 \cdot 2H_2O$ products obtained at different temperatures.

Effect of final pH. An increase in pH increases the Fe/P molar ratio (Fig. 8). However, increasing the pH with aqueous ammonia did not precipitate Fe and P in a 1:1 ratio, which would have indicated the production of $Fe(NH_4)_x(OH)_y(PO_4)_z \cdot nH_2O$. Increasing pH would precipitate more Fe^{3+} as $Fe(OH)_3$, resulting in more free $H_2PO_4^-/HPO_4^{2-}$, which then substituted the NH_4 or OH of $Fe(NH_4)_x(OH)_y(PO_4)_z \cdot nH_2O$, thereby slightly reducing the deviation from the Fe/P mole ratio. However, this process is less significant than the $Fe(OH)_3$ precipitation process, so Fe/P mole ratio increased as a result of the above factors. Therefore, the optimum pH was identified as 2.00.

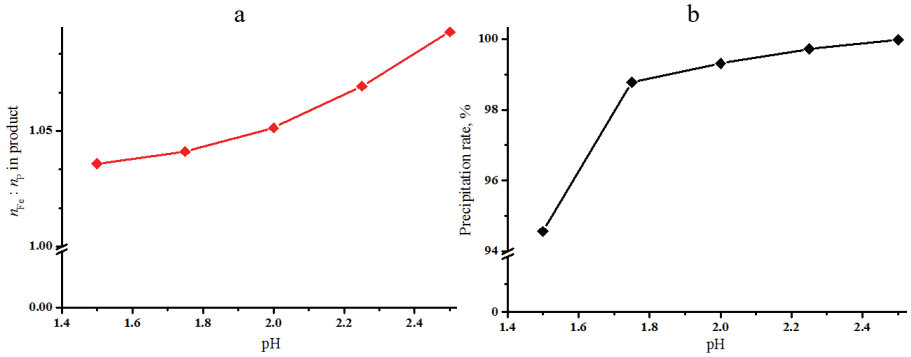

Fig. 8. a) Effect of pH on the Fe/P mole ratio in product; b) effect of pH on Fe precipitation rate.

Effect of the mole ratio of Fe:P in solution. The Fe/P mole ratio in the product decreased with the increase in the Fe/P mole ratio in the solution, because the $Fe(OH)_3$ produced in the solution would form $FePO_4 \cdot 2H_2O$ in the presence of excess $H_2PO_4^-/HPO_4^{2-}$ (Eq. (6)) and the excess of $H_2PO_4^-/HPO_4^{2-}$ would partially substitute the NH_4 or OH of the $Fe(NH_4)_x(OH)_y(PO_4)_z \cdot nH_2O$ and further reduce the Fe/P mole ratio (Fig. 9):

$$H^+ + Fe(OH)_3 + H_2PO_4^- \rightarrow FePO_4 \cdot 2H_2O + H_2O \quad (6)$$

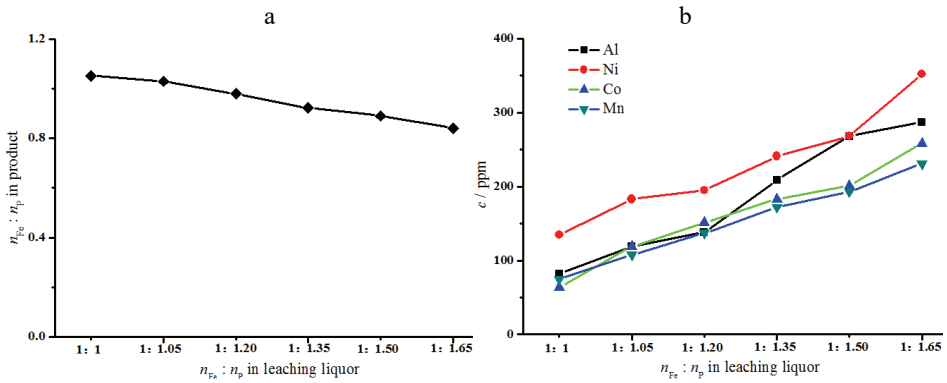

Fig. 9. a) Effect of Fe/P mole ratio in leached liquor on Fe/P mole ratio in product; b) effect of Fe/P mole ratio in leached liquor on Al, Ni, Co, and Mn content.

An increase in the Fe/P ratio led to an increase in the Ni, Co, Mn, and Al content in the product because the increase in the solution concentration of $H_2PO_4^-/HPO_4^{2-}$ results in precipitation of greater quantities of the insoluble phosphate salts of Ni, Co, Mn and Al, leading to increase in the Ni, Co, Mn and Al content in the product from Eqs. (7) and (8). Therefore, an Fe/P mole ratio 1:1.2 was selected as the optimal condition:

$$H_2PO_4^-/HPO_4^{2-} + Me^{2+} + OH^- \rightarrow Me_3(PO_4)_2\downarrow + H_2O \text{ (Me = Ni, Co, Mn)} \quad (7)$$

$$H_2PO_4^-/HPO_4^{2-} + Al^{3+} + OH^- \rightarrow AlPO_4\downarrow + H_2O \quad (8)$$

Effect of complexing agent. Increase in [EDTA-2Na] leads to a reduction in the Al, Ni, Co and Mn quantities in the product and slows the rate of precipitation of iron (Fig. 10). As [EDTA-2Na] is increased, the dianion effectively chelates divalent and trivalent ions such as Fe^{3+}, Al^{3+}, Ni^{2+}, Co^{2+} and Mn^{2+} result in the ions more present in the solution and it serves to reduce the Al, Ni, Co and Mn content in the product. This serves to reduce the Al, Ni, Co and Mn content in the product, however, the excess of EDTA-2Na decreases the iron precipitation rate due to complexation, and the process is shown in Eqs. (9)–(11). The precipitation rate of the product would be affected, and the subsequent recovery of Ni, Co, Mn and Li from the precipitating mother liquor would be more difficult. Therefore, a 20 g L^{-1} [EDTA-2Na] was selected as optimal. The chemical compositions met the battery requirements and the elemental contents as listed in Table V. Next, the particle size and morphology were adjusted:

$$3EDTA^{2-} + 2Fe^{3+} \leftrightarrows Fe^{III}_2(EDTA)_3 \quad (9)$$

$$3EDTA^{2-} + 2Al^{3+} \leftrightarrows Al_2(EDTA)_3 \quad (10)$$

$$EDTA^{2-} + Me^{2+} \leftrightarrows Me^{II}EDTA \text{ (Me = Ni, Co, Mn)} \quad (11)$$

Effect of ammonia addition rate. The particle size of $FePO_4{\cdot}2H_2O$ products gradually increased with the raise of ammonia addition time. As can be seen from

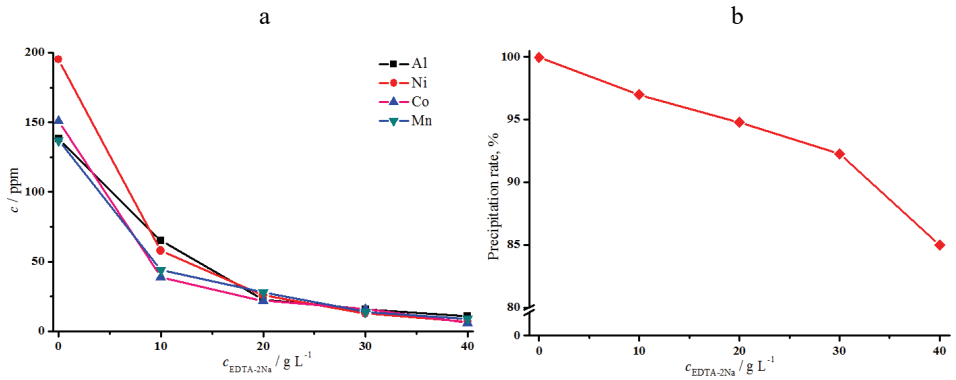

Fig. 10. a) Effect of EDTA-2Na addition on the content of Al, Ni, Co and Mn; b) effect of EDTA-2Na addition on the precipitation rate of Fe.

TABLE V. Chemical content of $FePO_4 \cdot 2H_2O$ obtained; $FePO_4 \cdot 2H_2O$ standard refers to standard HG/T 4701-2014

Component	Content, wt.%		Content, ppm					
	Fe	P	SO_4^{2-}	Al	Ni	Co	Mn	Li
Index	29.0–30.0	16.2–17.2	<100	---	<50	---	<1000	---
Content	29.81	16.88	32	22	21	25	16	5

Component	Content, ppm							Mole ratio
	Ca	Mg	Na	K	Cu	Zn	Cl^-	Fe / P
Index	<50	<50	<100	<100	<50	<50	<100	0.97–1.02
Content	13	5	21	2	21	10	92	0.98

Fig. 11, when the addition time reached 90 min, the particles of $FePO_4 \cdot 2H_2O$ were nearly spherical. In industry, the required particle size (D50) of the $FePO_4 \cdot 2H_2O$ product is 3±1 mm. Larger particle sizes result in incomplete solid-state reactions and excessively small particle sizes often result in low-density material (small particle size may cause agglomeration effects, in which primary particles first bond to each other to become loose secondary particles with densities smaller than those resulting from dispersed particles) and low specific capacity (the smaller the density of the material, the thicker the coating material must be to reach the corresponding capacity, when the battery is coated and fabricated, thus resulting in lower volumetric capacity).[27,28] Particles of the product should exhibit sizes within 50–200 nm range, but the particle size of $FePO_4 \cdot 2H_2O$ product obtained *via* single feeding methods could not be well-controlled and the primary particle size was 200–500 nm. At the same time, considering that the continuous operation would save costs in the industrialisation process, it is proposed that $FePO_4 \cdot 2H_2O$ products should be prepared *via* the concurrent feeding method.

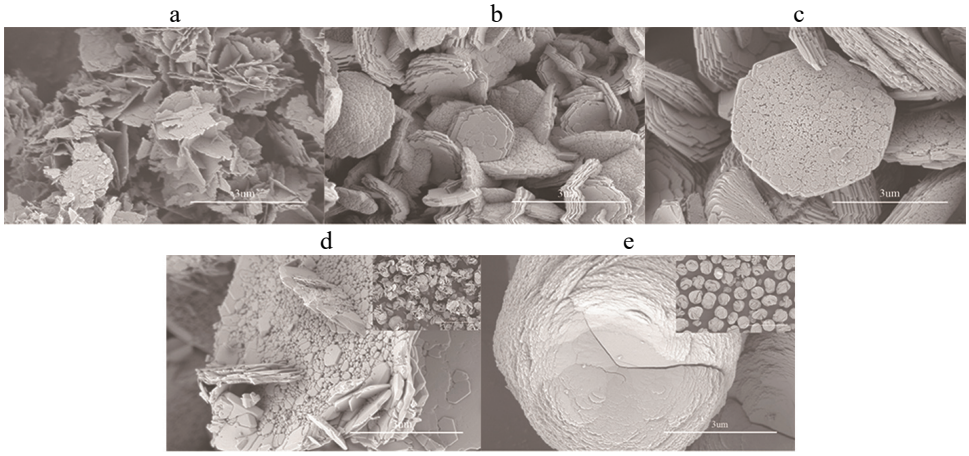

Fig. 11. Effect of ammonia addition time on morphology at 85 °C, final pH of 2, Fe/P mole ratio of 1:1.2 and 20 g L^{-1} EDTA-2Na: a) 10; b) 30; c) 50; d) 70; e) 90 min.

Effect of concurrent feeding speed. Fig. 12 showed that the product gradually changes from a spherical structure to a flake structure with the increases in the feeding rate of the prepared leaching liquid. It is also observed that increases in feeding speed lead to the decreases in the size of primary particles of $FePO_4{\cdot}2H_2O$, from 100–250 nm at a flow rate of 2–7 mL/min to 50–150 nm at a flow rate of 12–22 mL/min, while the particle size stabilised at 2–4 μm. When the rate of liquid feeding increased, the free Fe^{3+} in the slurry could not bind to the crystal seeds rapidly enough to form a precipitate and when nucleation rate was greater than growth rate, small crystal nuclei were formed and led to a red-

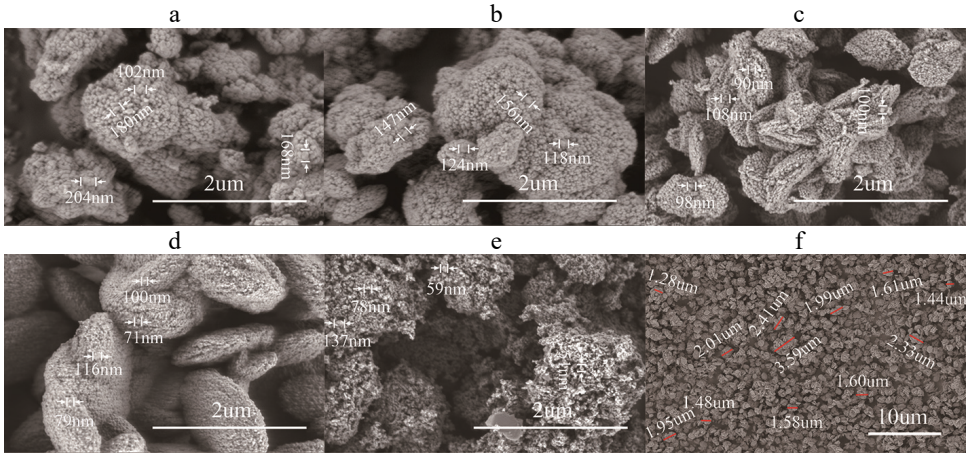

Fig. 12. Effect of concurrent feeding speed on morphology at 85 °C, final pH of 2, Fe/P mole ratio of 1:1.2 and 20 g L^{-1} EDTA-2Na: a) 2 mL/min, 100000×; b) 7 mL/min, 100000×; c) 12 mL/min, 100000×; d) 17 mL/min, 100000×; e) 22 mL/min, 100000×; f)12 mL/min, 10000×.

uction in primary particle size. The optimum feeding rate was selected as 12 mL/min based on the electron microscope images of the synthesised particles. The XRD patterns of $FePO_4·2H_2O$ product and $FePO_4$ product (from $FePO_4·2H_2O$ after heat treatment at 500 °C) are shown in Fig. 13. The product was confirmed to be $FePO_4·2H_2O$, which dried to $FePO_4$ after heat treatment.

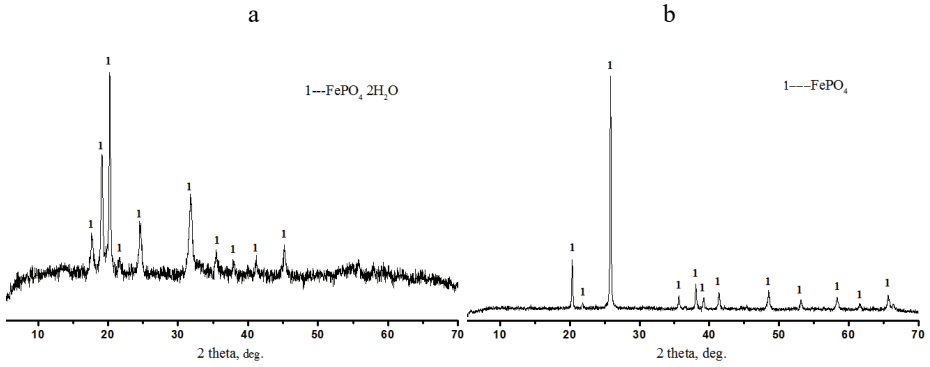

Fig. 13. XRD pattern of $FePO_4·2H_2O$ products: a) after drying at 80 °C; b) after heat treatment at 500 °C.

CONCLUSION

Proposed herein is a new method for recovering battery grade $FePO_4·2H_2O$ from $LiFePO_4/LiNi_xCo_yMn_{1-x-y}O_2$ mixed waste. The waste was leached with HCl and H_2O_2 first, and the optimum leaching occurred at a temperature of 50 °C, a liquid–solid ratio of 3:1, a HCl/raw material ratio of 1.96 ml g^{-1}, a H_2O_2/ /raw material ratio of 0.24 ml g^{-1}; a reaction time of 2 h. The optimum conditions for the precipitation from 1.0 M Fe leached solution were a pH of 2.0, a temperature of 85 °C, and a EDTA-2Na concentration of 20 g L^{-1}. Results also showed that a relatively slow ammonia addition rate of 12 mL/min and the concurrent feeding method favoured the formation of $FePO_4·2H_2O$. Under these conditions, the percentages of Ni, Co, Mn and Al obtained in the products were less than 50 ppm, and the particle size controlled at 1–5 μm (D50).

ИЗВОД

ДОБИЈАЊЕ $FePO_4·2H_2O$ ОД СМЕШЕ ОТПАДНИХ МАТЕРИЈАЛА $LiFePO_4$ и $LiNi_xCo_yMn_{1-x-y}O_2$

HONGHUI TANG[1,2], YANCHAO QIAO[2], XI DAI[1], FENG TAN[2] и QIANG LI[2]

[1]*School of Metallurgy and Environment, Central South University, 410083 Changsha, Hunan, P. R. China и*
[2]*Hunan Brunp Recycling Technology Co., Ltd, 410600 Ningxiang, Hunan, P. R. China*

У раду је развијен метод за добијање $FePO_4·2H_2O$, који се може користити за производњу батерија, полазећи од смеше отпадних материјала $LiFePO_4$ и $LiNi_xCo_yMn_{1-x-y}O_2$. Одређени су оптимални услови лужења: температура 50 °C, однос течно/чврсто = 3:1, молски однос $HCl/FePO_4·2H_2O$ = 3,6, молски однос $H_2O_2/FePO_4·2H_2O$ = 0,75 и реакционо време 2 h. Раствор добијен лужењем је разблажен до концентрације 1,0 M Fe и испити-

ван је утицај температуре, pH, комплексирајућег агенса, брзине додавања амонијака и начина мешања реагенаса на преципитацију, величину честица и морфологију $FePO_4{\cdot}2H_2O$. Велика брзина преципитације и мали садржај примеса Al, Ni, Co и Mn у $FePO_4{\cdot}2H_2O$ су постигнути када је преципитација извођена на 85 °C, pH 2 и при концентрацији комплексирајућег агеса од 20 g L^{-1}. Такође, утврђено је да споро додавање амонијака и начин мешања реагенаса утичу на добијање $FePO_4{\cdot}2H_2O$ малих величина честица, плочасте морфологије.

(Примљено 16. септембра 2019,ревидирано 10. јануара 2020, прихваћено 16. јануара 2020)

REFERENCES

1. C. W. Sun, R. Shreyas, J. B. Goodenough, F. Zhou, *J. Am. Chem. Soc.* **133** (2011) 2132 (https://doi.org/10.1021/ja1110464)
2. S. P. Wang, H. X. Yang, L. J. Feng, S. M. Sun, J. X. Guo, Y. Z. Yang, H. Y. Wei, *J. Power Sources* **233** (2013) 43 (https://doi.org/10.1016/j.jpowsour.2013.01.124)
3. Y. X. Gu, W. M. Liu, W. Lei, G. C. Li, Y. Yu, *Crystengcomm* **15** (2013) 4865 (http://doi.org/10.1039/C3CE00072A)
4. Q. Wang, S. X. Deng, H. Wang, M. Xie, J. B. Liu, H. Yan, *J. Alloys Compd.* **553** (2013) 69 (https://doi.org/10.1016/j.jallcom.2012.11.041)
5. F. Y. Cheng, J. Liang, Z. L. Tao, J. Chen, *Adv. Mater.* **23** (2011) 1695 (https://doi.org/10.1002/adma.201003587)
6. B. Scrosati, J. Garche, *J. Power Sources* **195** (2009) 2419 (https://doi.org/10.1016/j.jpowsour.2009.11.048)
7. B. Scrosati, J. Hassoun, Y. K. Sun, *Energy Environ. Sci.* **4** (2011) 3287 (https://doi.org/10.1039/C1EE01388B)
8. Y. Zhang, Q. Y. Huo, P. P. Du, L. Z. Wang, A. Q. Zhang, Y. H. Song, Y. Lv, G. Y. Li, *Synth. Metals* **162** (2012) 1315 (https://doi.org/10.1016/j.synthmet.2012.04.025)
9. J. J. Wang, X. L. Sun, *Energy Environ. Sci.* **5** (2012) 5163 (https://doi.org/10.1039/C1EE01263K)
10. X. Wang, G. Gaustad, C. W. Babbitt, K. Richa, *Resour. Conserv. Recycl.* **83** (2014) 53 (https://doi.org/10.1016/j.resconrec.2013.11.009)
11. J. Chen, Y. C. Zou, F. Zhang, Y. C. Zhang, F. F. Guo, G. D. Li, *J. Alloys Compd.* **563** (2013) 264 (https://doi.org/10.1016/j.jallcom.2013.02.131)
12. G. Q. Cai, K. Y. Fung, K. M. Ng, C. Wibowo, *Ind. Eng. Chem. Res*. **53** (2014) 18245 (https://doi.org/10.1021/ie5025326)
13. L. Han, D. L. He, A. J. Liu, D. M. Ma, *Chin. J. Power Sources* **38** (2014) 548 (https://doi.org/CNKI:SUN:DYJS.0.2014-03-051)
14. S. Barusseau, B. Beder, M. Broussely, F. Perton, *J. Power Sources* **54** (1995) 296 (https://doi.org/10.1016/0378-7753(94)02087-J)
15. P. G. Bruce, S. Bruno, T. Jean-Marie, *Angew. Chem. Int. Ed.* 47 (2008) 2930 (https://doi.org/10.1002/anie.200702505)
16. X. T. Jiang, P. Wang, L. H. Li, J. Yu, Y. X. Yin, F. Hou, *Mater. Sci. Forum* **943** (2019) 141 (https://doi.org/10.4028/www.scientific.net/MSF.943.141)
17. N. Omar, M. A. Monem, Y. Firouz, J. Salminen, J. Smekens, O. Hegazy. H. Gaulous, G. Mulder, P. V. D. Bossche, T. Coosemans, J. V. Mierlo, *Appl. Energy* **113** (2013) 1575 (https://doi.org/10.1016/j.apenergy.2013.09.003)
18. L. X. Yuan, Z. H. Wang, W. X. Zhang, X. L. Hu, J. T. Chen, Y. H. Huang, J. B. Goodenough, *Energy Environ. Sci.* **4** (2010) 269 (https://doi.org/10.1039/c0ee00029a)

19. X. L. Li, J. Zhang, D. W. Song, J. S. Song, L.Q. Zhang, *J. Power Sources* **345** (2017) 78 (https://doi.org/10.1016/j.jpowsour.2017.01.118)
20. H. Tanaka, A. Yasukawa, K. Kandori, T. Ishikawa, *Colloids Surfaces, A* **204** (2002) 251 (https://doi.org/10.1016/S0927-7757(02)00005-5)
21. N. K. Mal, A. Bhaumik, M. Matsukata, M Fujiwara. *Ind. Eng. Chem. Res*. 45 (2006) 7748 (https://doi.org/10.1021/ie060609u)
22. D. C. Bian, Y. H. Sun, S. Li, Y. Tian, Z. H. Yang, X. M. Fan, W. X. Zhang, *Electrochim. Acta* **190** (2015) 134 (https://doi.org/10.1016/j.electacta.2015.12.114)
23. Y. X. Yang, X. H. Zheng, H. B. Cao, C. L. Zhao, X. Lin, P. G. Ning, Y. Zhang, W. Jin, Z. Sun, *ACS Sustain. Chem. Eng.* **5** (2017) 9972 (https://doi.org/10.1021/acssuschemeng.7b01914)
24. B. Dong, G. Li, X. G. Yang, L. M. Chen, G. Z. Chen, *Ultrason. Sonochem.* **42** (2018) 452 (https://doi.org/10.1016/j.ultsonch.2017.12.008)
25. W. P. He, L. P. Xue, B. Gorczyca, J. Nan, Z. Shi, *Sep. Purif. Technol.* **190** (2018) 228 (https://doi.org/10.1016/j.seppur.2017.08.063)
26. A. Tamburini, G. Gagliano, G. Micale, A. Brucato, F. Scargiali, M. Ciofalo, *Chem. Eng. Sci.* **192** (2018) 161 (https://doi.org/10.1016/j.ces.2018.07.023)
27. D. M. Zheng, H. Z. Pan, L. P. Wu, J. C. Chen, J. H. Peng, Chin. *J. Power Sources* **39** (2015) 58 (https://doi.org/10.3969/j.issn.1002-087X.2015.01.017)
28. Z. M. Ma, R. G. Xiao, X. Liao, X. Ke, *Mater. Rev*. **32** (2018) 3325 (https://doi.org/10.11896/j.issn.1005-023X.2018.19.006).